Interfaces in spinor Bose-Einstein condensates

Jurre Corver
Utrecht University

Supervisor: Prof. dr. ir. H.T.C. Stoof
January 14, 2015

Abstract

Bose-Einstein condensates - a state of matter at low temperature in which a macroscopic amount of bosons occupy the quantum-mechanical ground state- were originally trapped magnetically. The drawback of this trapping method is that only the weak-field seeking spin state is trapped and we therefore only have a one component i.e. scalar condensate. In contrast, optical trapping confines atoms of all spin state and therefore allows for spin degrees of freedom, resulting in spinor Bose Einstein condensates. In this thesis, density profiles of these spinor condensates have been calculated in Thomas-Fermi approximation. The profiles show areas with strict phase separation, but also areas with spin mixtures. For sodium atoms we get a strict separation between the $m_F = \pm 1$ and the $m_F = 0$ spin state in Thomas-Fermi approximation. This however causes discontinuities in the transition between spin domains and thus these interfaces were studied further. We found that the density profile of a spin state behaves roughly like a hyperbolic tangent at such an interface. Finally, a differential equation is proposed that could be solved as a starting point of follow-up research.

Contents

1 Introduction

1.1 History

In 1924 it was predicted by Albert Einstein and Satyendra Bose that a phase transition occurs at temperatures close to absolute zero, in which a macroscopic amount identical particles with integer spin occupy the ground state[1]. The particles are now called bosons and the phenomenon Bose-Einstein condensation(BEC). It was not until 1995 that BEC found experimental verification for dilute atomic gases of rubidium cooled to 170 nK by Eric Cornell and Carl Wieman of the JILA institute. In 2001 they shared at Nobel price with Wolfgang Ketterle of MIT, who realized a condensate of Sodium particles 4 months later as well as doing fundamental research on Bose-Einstein condensation. Enabling this research was the combination of the technique of laser cooling and evaporative cooling in a magnetic trap, of which the realization of the first of these techniques was also awarded a Nobel price in 1997.

Following its first experimental realization was a great surge of both experimental and theoretical research in the field of Bose-Einstein condensation. This is because it enables us to study quantum phenomena more closely as well as provide some interesting applications, of which the most notable is possibly quantum computing. But there are also benefits for different fields. For instance, the trapping of BEC particles in an optical lattice simulates the crystalline structures that solid-state physicists work with, but in BEC the conditions can be controlled much more easily.

Amidst all of these intriguing aspects of in the field of Bose-Einstein condensation, is a special field concerning condensates with atomic spin degrees of freedom: spinor Bose-Einstein condensates. We can consider them as multi-component BECs with some special properties. For instance, the number of particles per spin state is not conserved, since particles can change spin as long as the total spin number is conserved and quantum phenomena like spin-mixing, spin waves and spin dynamics occur. On top of that there is also a dependence on the quadratic Zeeman effect. This differentiates these condensates from regular BECs or mixtures of different type of particles in one BEC. Both spin-1 and spin-2 spin condensates have been prepared, and it is expected that more research will be done in the future.

1.2 Cooling techniques

In order to fabricate a BEC, one of the most important elements is to cool our sample as much as possible. Two important techniques form the basis of this cooling process and will be briefly discussed below.

1.2.1 Laser Doppler cooling

As we know, the energy of a photon is given by $E = \hbar\nu$ where $\hbar$ is the reduced Planck constant and ν the frequency. Suppose a particle has a velocity $\mathbf{v} = v\hat{\mathbf{v}}$ in the lab frame. We introduce two laser beams derived from the same source such that they have the same energy in the lab frame, one pointing at the particle in direction $\hat{\mathbf{v}}$ and the other pointing at the particle in direction $hat\mathbf{v}$. When the photon hits the particle, momentum will be exchanged such that the speed of the particle will change according to $\delta v_P = \frac{p_l}{m_p}$ with $p_l = \frac{\hbar}{\lambda}$ the momentum of the photon and m_p the weight of the particle.

If the particle is at rest in the lab frame, nothing will happen as the same force is applied in both directions. If however $v \neq 0$, Doppler shift will cause a difference in both forces such that the particle will be slowed close to zero velocity in the lab frame. We have to also keep in mind that a particle will only absorb a photon if it is within a certain Lorentzian shaped frequency band. We have to tune the lasers accordingly. If we do this on a macroscopic scale, we have effectively cooled our sample down. An image elucidating this process is shown in figure 1 Temperatures as low as $35\mu K$ have been achieved using this technique on a sample of sodium [2].

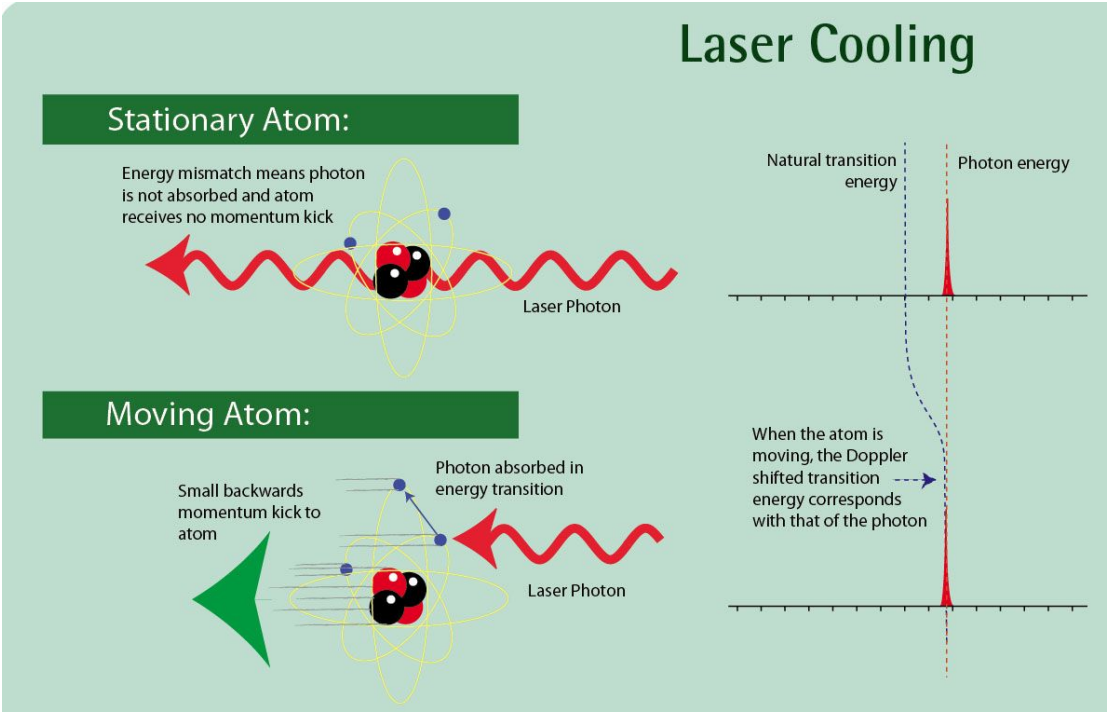

Figure 1 – Self explanatory image elucidating the technique of laser cooling. Taken from the website of the Australian national university [3]

1.2.2 Evaporative cooling

After the atoms have been laser-cooled, evaporative cooling will be used to reach the critical temperature for Bose-Einstein condensation. The technique of evaporative cooling will be explained on the basis of figure 2. Suppose a group of atoms is trapped in an optical or magnetic trapping potential like in part (a) of the image. Just like with evaporation, high energetic particles can escape this potential thus lowering the average energy of the atoms in the trap. We can then gradually lower the potential as shown in part (b) and (c) of the image. Again the most energetic atoms will escape the trap. The remaining atoms will exchange momentum through collisions and thus reach a new lower temperature equilibrium. This process is called rethermalization. After all atoms are rethermalized, we can keep repeating this process until the critical temperature is reached.

1.3 Spinor Bose-Einstein condensates

As has been discussed, a Bose-Einstein condensate is a state of matter in which a non-zero fraction of particles occupy the ground state. Using the cooling techniques discussed in last paragraph, we can reach temperatures low enough for Bose-Einstein condensation to occur. As shown in figure 3, hyperfine splitting causes different energy levels for different values of the total angular momentum quantum number F. If we choose a magnetic trapping potential, only the atoms in the weak-field seeking spin state will be trapped, thus giving as a single component BEC [5]. We will refer to these single component condensates as scalar Bose-Einstein condensates. If however we would use an optical trap, the hyperfine splitting will not occur since we are not using any magnetic field. In this way, an optical trap can confine all spin components, which is crucial for creating a spinor Bose-Einstein condensate: a Bose-Einstein condensate with different spin components. Spinor BECs will be the main focus of this paper.

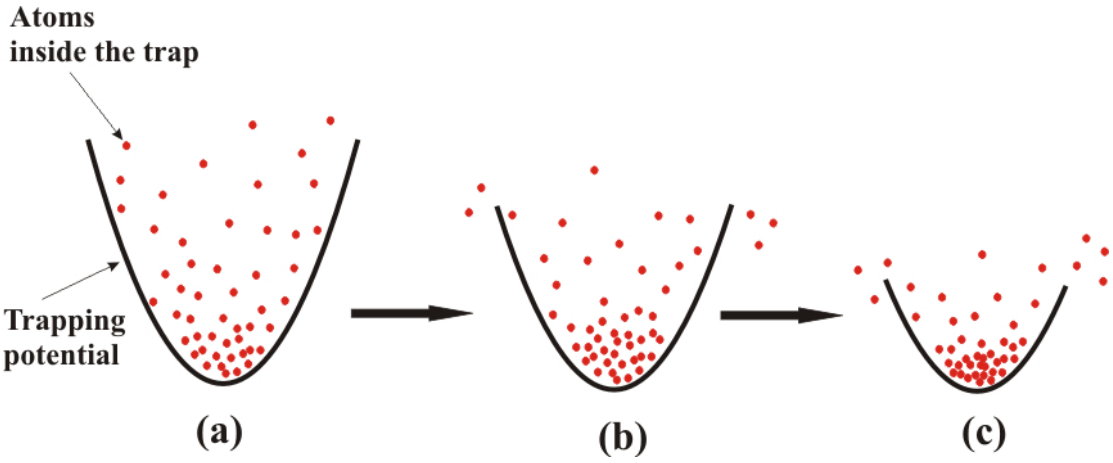

Figure 2 – Image explaining the process of evaporative cooling. Taken from the website of the university of Michigan [4]

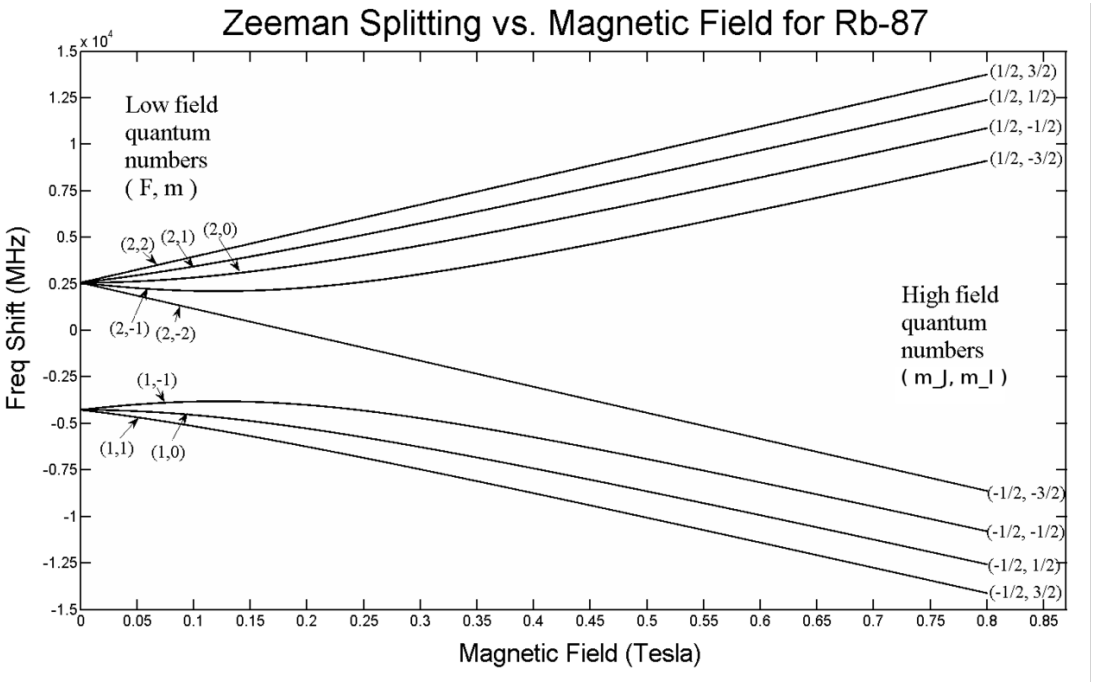

Figure 3 – Image showing Zeeman splitting of the 5s level of Rb-87 as an illustration of this effect. Here $F = J + I$ where I is the nuclear spin, J is the total electronic angular momentum and F is the total angular momentum of the atom. [6]

1.4 Outline

In chapter 2, a general theory of Bose-Einstein condensates will be developed. In this theory we will derive some general properties that are needed for a BEC to exist, like critical temperature and the energy equation for a BEC. In chapter 3, this information will be used to derive density equations for spinor Bose-Einstein condensates in one dimension using the Thomas-Fermi approximation which will be introduced in the same chapter. Here, it will be assumed that the condensate has the temperature of absolute 0. In chapter 4, results in chapter 3 will be improved by studying the interface between a spin -1 domain and a spin 0 domain. Finally, it will be shown how numerical methods can be used to enhance these results.

2 Bose-Einstein condensates

Predicted in 1924 and only experimentally realized in 1995, the Bose-Einstein condensate in dilute atomic gases is a fairly new discovery. BEC of many atoms have been made, for instance ^{1}H, ^{7}Li, ^{23}Na, ^{85}Rb, ^{87}Rb and ^{133}Cs. Putting these atoms into optical lattices has provided condensed matter physicists with the opportunity to study many body systems more easily, for it is easy to manipulate the condensate.

As a gas gets colder, a greater proportion of its atoms will occupy the lower energy state as described by the Bose-distribution in paragraph 2.1. If the gas reaches its critical temperature T_c derived in paragraph 2.2 , a non zero fraction of the atoms will occupy the ground state. These atoms in the ground state can now be described by the same wave function and together they share some of the same properties a single atom has, hence the term "superatom" was coined. Using the Gross-Pitaevskii equation derived in paragraph 2.5, we can now find the wave function that describes the density profile of this gas.

These quantum gases deviate from ordinary gases in some properties. They have a density of about 10^{13}-10^{15} particles a cm^{-3} as opposed to the density of molecules in air at room temperature and atmospheric pressure of order 10^{19} particles a cm^{-3} and in liquids and solids of order 10^{22}cm^{-3}[7]. Next to that temperatures have to be of the order of 10^{-5}K or less in combination with densities like this for quantum phenomena to occur. This is contrasted with quantum effect in liquid helium or order 1 K and quantum effects for electrons in metal below the Fermi temperature of around 10^{4}-10^{5} K. As we know, bosons are integer spin particles. Their wave functions are symmetric under exchange of every two particles, unlike that of a fermion. Therefore, bosons can occupy the same quantum state such that it is possible to find many bosons in the ground state. This fact is essential for Bose-Einstein condensation. In this chapter we will derive some fundamental properties of the BEC.

2.1 Bose distribution

One of the fundamental frameworks that describe Bose-Einstein condensation is the Bose-Einstein distribution or Bose distribution. This statistical formula describes a quantum system of non-interacting and indistinguishable bosons. It gives us the amount of particles N in an energy state as a function of the energy ϵ. We will derive it from the grand canonical ensemble, in which the system is allowed to exchange particles with a reservoir.

Using the properties of indistinguishability and non-interactivity, we can consider every energy level ϵ as a separate thermodynamic system in contact with a reservoir[8]. In other words, we can find a distribution for the amount of particles per energy level. Each energy level corresponds to one micro state due to indistinguishability and for bosons therefore there is no limit to the amount of particles per energy state. Using the known results of the geometric series results in the following partition function

$$Z = \sum_{N=0}^{\infty} \exp \beta N(\mu - \epsilon) = \frac{1}{1 - e^{\beta(\mu-\epsilon)}} \tag{1}$$

From this partition function, we can easily calculate the expected value for the mount of particles N.

$$< N >= \frac{1}{\beta} \ln \left(\frac{\partial Z}{\partial \mu} \right)_{V,T} = \frac{1}{e^{\beta(\epsilon-\mu)} - 1} \equiv f(\epsilon) \tag{2}$$

A plot of this so called Bose distribution is shown in figure 4. Note that it is valid for every energy level and that it approximates the Boltzmann distribution for high temperatures.

2.2 Critical temperature and Bose-Einstein condensation

In the previous paragraph we derived an equation for the expected amount of particles N as a function of the energy of a certain state. In this paragraph, we will use this equation to understand some of requirements of Bose-Einstein condensation. Denote the ground state - the

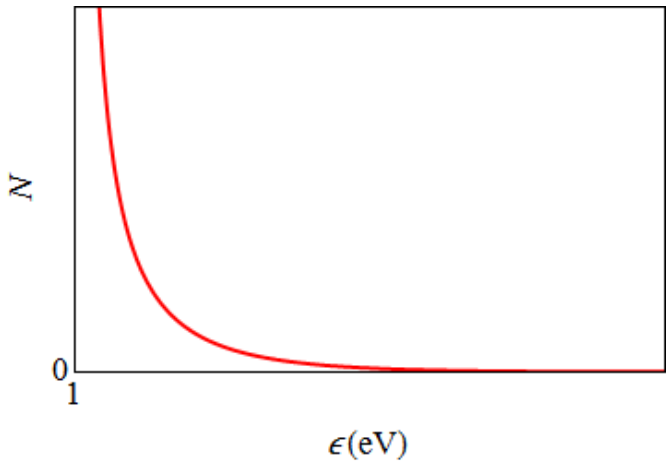

Figure 4 – Plot of Bose distribution for $\mu = k_B T = 1$. Notice that the function goes to infinity as ϵ goes to $\mu = 1$.

lowest value for ϵ - as ϵ_{min}. If $\mu > \epsilon_{min}$ then the expected amount of particles N takes a negative value according to equation 2. Because this is unphysical, we require that $\mu \leq \epsilon_{min}$. We are interested in knowing the amount of particles that populate the ground state N_0. We can find this by calculating the total number of particles in the excited state N_{ex} and subtracting it from the total number of particles N_T such that $N_0 = N_T - N_{ex}$. If we find a macroscopic amount of particles in the ground state, then it we can say the system has a Bose-Einstein condensate. Note that for larger T, μ decreases.

2.3 BEC in anisotropic harmonic-oscillator potential

We will now calculate the critical temperature for a k-dimensional harmonic potential $V(\mathbf{r}) = \frac{m}{2}\sum_{i=1}^{k}(\omega_i x_i^2)$ with Hamiltonian operator $\hat{H} = \frac{\hat{\mathbf{p}}^2}{2m} + V$. Using ladder operators we can then derive that the energy levels are given by

$$\epsilon(n_1, n_2, ..., k) = \sum_{i=1}^{k} \hbar\omega_i(n_i + \frac{1}{2}) \tag{3}$$

. Here n_i are integers greater than or equal to 0.

We are now going to determine the number of states $G(\epsilon)$ that have energy smaller than ϵ. If the energy is large compared to $\hbar\omega_i$, we can to a very good approximation treat n_i as a continuous variable and neglect the ground state. Motivated by equation 3, we define $\epsilon_i = \hbar\omega(n_i + \frac{1}{2})$ such that $\mathrm{d}n_i = \frac{d\epsilon_i}{\hbar\omega_i}$ Noting that $\epsilon = \epsilon_1 + ... + \epsilon_k$ is the surface of constant energy, we integrate over all positive values of ϵ_i such that

$$\begin{aligned} G(\epsilon) = \frac{1}{\hbar^k \prod_{i=1}^{k}\omega_i} \int_0^{\epsilon} \mathrm{d}\epsilon_1 \int_0^{\epsilon-\epsilon_1} \mathrm{d}\epsilon_2 ... \int_0^{\epsilon-\epsilon_1-...-\epsilon_k} \mathrm{d}\epsilon_k \\ = \frac{\epsilon^k}{k!\prod_{i=1}^{k}\omega_i} \end{aligned} \tag{4}$$

The density of states is then given by

$$g(\epsilon) = \frac{\epsilon^{k-1}}{(k-1)!\prod_{i=1}^{k}\omega_i} \equiv C_k \epsilon^{k-1} \tag{5}$$

Finally, using this information we can calculate the amount of particles in the excited state

$$N_e x = \int_0^{\infty} \mathrm{d}\epsilon g(\epsilon) f(\epsilon) \tag{6}$$

This integral is maximal for $\mu = 0$, so we pick this value. The transition temperature is defined as the temperature on which the total number of particles can just exist in the ground state and thus. – transform to x!!!!

$$N = C_k(K_b T_c)^k \int_0^\infty \mathrm{d}x \frac{x^{k-1}}{e^x - 1} \tag{7}$$

Solving this integral and noting that $\Gamma(k) \equiv= \int_0^\infty t^{k-1} e^{-t} \mathrm{d}t$ is the gamma function, one can prove by partial integration that $\Gamma(k) = (k-1)!$ if $k \in \mathbb{N}$ and note that $\zeta(k) = \sum_{n=1}^\infty n^{-k}$ the Riemann-zeta function. We solve the integral in equation 7 by taylor expanding the Bose distribution in terms of e^{-x}, such that

$$\begin{aligned} \int_0^\infty \mathrm{d}x \frac{x^{k-1}}{e^{x-1}} &= \int_0^\infty \mathrm{d}x x^{k-1} \sum_{n=1}^\infty e^{-nx} \\ &= \sum_{n=1}^\infty \int_0^\infty \mathrm{d}x \frac{(nx)^{k-1}}{n^{k-1}} e^{-nx} \\ = \sum_{n=1}^\infty \frac{1}{n^k} \int_0^\infty \mathrm{d}t t^{k-1} e^{-t} &= \zeta(k)\Gamma(k) \end{aligned} \tag{8}$$

Note that ζ diverges for $k \leq 1$. This means that there is no macroscopic fractions of particles in the ground state and therefore the only Bose-Einstein condensate that exists in this situation is one at temperature $T = 0$. Using this equation, we can now calculate the critical temperature:

$$k_B T_c = \frac{N^{\frac{1}{k}}}{(C_k \Gamma(k) \zeta(k))^{\frac{1}{k}}} \tag{9}$$

The Riemann-zeta function has exact values for even k and can be approximated for easily for other values. This formula proves that for the case of a harmonic potential in 1 dimension i.e. $k = 1$, Bose-Einstein condensations only occurs for $T = 0$.

Finally, it is interesting to know the fraction of of particles in the excited state. Combining equation 7 and 8 gives us that

$$N_{ex} \equiv N_T \left(\frac{T}{T_C} \right)^k \tag{10}$$

together with the fact that $N_0 = N_T - N_{ex}$, we end up with a fraction for the amount of particles in the ground state:

$$\frac{N_0}{N_T} = n_0 = 1 - \left(\frac{T}{T_C} \right)^k \tag{11}$$

for $T \leq T_0$ and $k > 1$. Note that the fraction at $T = T_C$ is still 0 as required, and that also n_0 tends to 1 as T tends to 0, as expected.

2.4 Interactions

In dilute gases, interatomic interaction is very unlikely because the range of interaction is small compared to the separation. When however a pair of atoms do interact, the resulting forces are strong. The configuration of such a system is constantly changing and that makes it hard to calculate each interaction. This can however be avoided by introducing an effective two body interaction U_{eff}. We will now consider two particles from their center of mass frame with reduced mass m_r. To first order in the interaction, the scattering length is given by

$$a_{Born} = \frac{m_r}{2\pi\hbar^2} \int \mathrm{d}\mathbf{r} U(\mathbf{r}), \tag{12}$$

which we call the Born approximation[7]. After this assumption, which we shall treat as an axiom, it is easy to see that

$$\int \mathrm{d}\mathbf{r} U_{eff}(\mathbf{r}) = \frac{2\pi\hbar^2 a}{m_r} = \frac{4\pi\hbar^2 a}{m} \equiv U_0. \tag{13}$$

Here we used that for particles with equal mass, $m_r = m/2$.

In our case of cold atoms, the complicated interatomic interaction can be replaced by an effective interaction that is proportional to the scattering length. In our model, atoms only interact when they are very close, which approximately means they should have the same position. We can therefore replace our potential by one of the following form

$$U_{eff}(\mathbf{r}, \mathbf{r}') = U_0 \delta(\mathbf{r} - \mathbf{r}') \tag{14}$$

with δ the Dirac delta. This final identity will be used in next paragraph to construct the hamiltonian for a BEC.

2.5 The Gross-Pitaevskii equation

In the previous paragraphs we have discussed that a Bose-Einstein condensate is obtained from a collection of bosons very close to the absolute 0 of temperature. Therefore, it is interesting to know more about the ground state energy of the system. In a dilute gas with particles of the same species, we can say that particles only interact with each other when they have the same location, so we can model this behavior with the Dirac delta as discussed in previous paragraph. Just like a hard sphere potential with radius zero, for which the potential is U_0. In addition we also have the standard kinetic energy term and we will add an external potential or trap potential V_{ext} to the equation. Therefore, the Hamiltonian operator of this system becomes:

$$\hat{H} = \sum_{i=1}^{N} \left(\frac{\mathbf{p_i^2}}{2m} + V_{ext}(\mathbf{r_i}) \right) + \frac{U_0}{2} \sum_{i=1}^{N} \sum_{j \neq 1}^{N} \delta(\mathbf{r_i} - \mathbf{r_j}) \tag{15}$$

Here $U_0 = \frac{4\pi\hbar^2 a_{ij}}{m}$ where a_{ij} is the scattering length that can be determined in experiments. Notice that for the first 2 terms we sum over all N particles of the system, and the final term is a summation over all pairs of particles, for which we have to divide U_0 by 2 as to not count the pairs double. Now, since we have a BEC, we can to a good approximation assume that all particles are in the same state: the ground state. Therefore, we can write in mean field approximation that

$$\psi(\mathbf{r_1}, \mathbf{r_2}, ..., \mathbf{r_N}) = \prod_{i=1}^{N} \zeta(\mathbf{r_i}) \tag{16}$$

And we can define that $\zeta(r)$ is normalized at 1 and we can define $\Psi = \sqrt{N}\psi$, which makes $|\Psi|^2$ normalized at the total number of particles N. The mean field approximation is valid when the gas is dilute. Otherwise, the interactions with the particles that are closer would be much stronger than the ones that are far away. We now want to minimize the free energy $F = E - \mu N$ or $F(\Psi) = \frac{\langle \Psi | \hat{H} | \Psi \rangle}{\langle \Psi \mid \Psi \rangle} - \mu \langle \Psi \mid \Psi \rangle$. Using the wave function Ψ, we can calculate the energy according to [12]

$$E = \frac{\langle \Psi | \hat{H} | \Psi \rangle}{\langle \Psi \mid \Psi \rangle} = \langle \psi | \hat{H} | \psi \rangle \tag{17}$$

Firstly, we calculate E. We know that $\hat{p} = \frac{\hbar}{\iota} \nabla$ such that

$$\langle \psi | \sum_{i=1}^{N} \frac{\mathbf{p_i^2}}{2m} | \psi \rangle = \frac{\hbar^2 N}{2m} \int \mathrm{d}\mathbf{r} |\nabla \zeta(\mathbf{r})|^2 \tag{18}$$

Now the term with the external potential becomes

$$\langle\psi| \sum_{i=1}^{N} V_{ext} |\psi\rangle = N \int \mathrm{d}\mathbf{r} \zeta^*(\mathbf{r}) V_{ext} \zeta(\mathbf{r}) \tag{19}$$

And finally the term with the interaction potential can be written as

$$\begin{aligned} &\langle\psi| \frac{U_0}{2} \sum_{i=1}^{N} \sum_{j\neq 1}^{N} \delta(\mathbf{r_i} - \mathbf{r_j}) |\psi\rangle \\ &= \frac{N(N-1)}{2} U_0 \int \mathrm{d}\mathbf{r_1} \int \mathrm{d}\mathbf{r_2} \zeta^*(\mathbf{r_1}) \zeta^*(\mathbf{r_2}) \mathbf{r_2} \delta(\mathbf{r_1} - \mathbf{r_2}) \zeta(\mathbf{r_1}) \zeta(\mathbf{r_2}) \\ &= \frac{N(N-1)}{2} U_0 |\zeta(\mathbf{r})|^4 \end{aligned} \tag{20}$$

We can combine all this equations to get an equation for the energy as a function of the wave function $\Psi(\mathbf{r}) = \sqrt{N}\psi(\mathbf{r})$. If we use that N is big, such that $N - 1 \approx N$, this results in the following energy functional:

$$E(\Psi) = \int \mathrm{d}\mathbf{r} \left(\frac{\hbar^2}{2m} |\nabla\Psi(\mathbf{r})|^2 + V_{ext}(\mathbf{r}) |\Psi(\mathbf{r})|^2 + \frac{1}{2} U_0 |\Psi(\mathbf{r})|^4 \right) \tag{21}$$

Note that $N = \int \mathrm{d}\mathbf{r} |\Psi|^2$ is constant. Taking this into account we should minimize the free energy $F(\Psi) = \frac{\langle\Psi|\hat{H}|\Psi\rangle}{\langle\Psi \mid \Psi\rangle} - \mu \langle\Psi \mid \Psi\rangle$. This free energy can be written as

$$F(\psi) = \int \mathrm{d}\mathbf{r} \left(\frac{\hbar^2}{2m} |\nabla\Psi(\mathbf{r})|^2 + (V_{ext}(\mathbf{r}) - \mu) |\Psi(\mathbf{r})|^2 + \frac{1}{2} U_0 |\Psi(\mathbf{r})|^4 \right) \tag{22}$$

Which is an equation that will often be used. We can now minimize this equation by taking the functional derivative to ψ^*. For instance

$$\begin{aligned} \frac{\delta \langle\Psi \mid \Psi\rangle}{\delta\psi^*} &= N \left(\int \mathrm{d}\mathbf{r} \psi^*(\mathbf{r}) \psi(\mathbf{r}) \right)^{N-1} \int \mathrm{d}\mathbf{r} \psi(\mathbf{r}) \\ &= N \int \mathrm{d}\mathbf{r} \psi(\mathbf{r}) \end{aligned} \tag{23}$$

Doing this for all terms and putting them to 0, gives us the well known time independent Gross-Pitaevskii equation.

$$\left(-\frac{\hbar^2}{2m} \nabla^2 + V_{ext}(\mathbf{r}) + \frac{4\pi\hbar^2 a_s}{m} |\Psi(\mathbf{r})|^2 \right) \Psi(\mathbf{r}) = \mu\Psi(\mathbf{r}) \tag{24}$$

Here we chose $U_0 = \frac{4\pi\hbar^2 a_{ij}}{m}$ where a_{ij} is the scattering length that has been determined experimentally. From next chapter onwards, Ψ will always be referred to as ψ, as is standard notation. Because the old ψ definition of ψ will not be used anymore, this should not cause too much confusion.

3 Spinor Bose-Einstein condensates

In the first gaseous BEC that was created, atoms in a single spin state of rubidium-87 were used. In these systems a magnetic trap was utilized in which only atoms in a week field seeking state were trapped and therefore their spin degrees of freedom are frozen. In optical traps however, spin internal degrees of freedom are not frozen which allows for spinor Bose-Einstein condensates i.e. BECs with spin degrees of freedom to exist.The first spinor BEC was created in 1998, just three years after the creation of the first BEC and was realized in a gas of spin-1 ^{23}Na particles.

As a result of the degrees of freedom in spin, there are now $2F + 1$ components in the BEC. These result in a rich variety of phases governed by different spin textures, which is extended because of the Zeeman effect when a magnetic field is introduced. Spin dynamics makes it possible to switch between spin states, as long as the total spin is conserved. Via a spin-exchange collisions in a spin-1 spinor BEC, a particle with magnetic spin number $M_F = 1$ and one with $M_F = -1$ can collide resulting in 2 $M_F = 0$ particles and vice versa and in this way a spinor BEC differentiates itself from other multi-component condensates.

3.1 Free energy equation: spin-1 BEC

In this paragraph, we will derive a phase diagram for the general case of a $F = 1$ spinor Bose-Einstein condensate. To do this we will use the Gross-Pitaevskii equation together with an the energy functional derived in paragraph 2.5.These results can be extended to describe the spin-1 spinor BEC. The difference with a standard BEC is that the scattering lengths a_{ij} may be different for every particle interaction. This constant may be different for interaction between $m_F = 1$,$m_F = 0$ and interactions between to particles with $m_F = 1$ etc. In other words, $a_{1,0} \neq a_{1,1}$. For this reason, U_0 is different for different particle interactions. We therefore now have to deal with a three component system.

For a $F = 1$ spinor BEC, our wave function can be described by the following vector

$$\psi(\mathbf{r}) = \begin{pmatrix} \psi_\uparrow(\mathbf{r}) \\ \psi_0(\mathbf{r}) \\ \psi_\downarrow(\mathbf{r}) \end{pmatrix} \tag{25}$$

In which we denoted $\psi_1(\mathbf{r}) = \psi_\uparrow(\mathbf{r})$ and $\psi_{-1}(\mathbf{r}) = \psi_\downarrow(\mathbf{r})$

.

We can therefore write the result for the free-energy functional taking into account every single component:

$$F = \int \mathrm{d}x \left(\sum_{i\in\{-1,0,1\}} \frac{\hbar^2}{2m} |\nabla\psi_i(\mathbf{r})|^2 + (V - \mu_i)|\psi_i(\mathbf{r})|^2 + \frac{1}{2} \sum_{i,j\in\{-1,0,1\}} g_{i,j}|\psi_i(\mathbf{r})|^2|\psi_j(\mathbf{r})|^2 \right) \tag{26}$$

If however the number of particles in a gas is very large, the interatomic interaction becomes very large such that the kinetic energy term can be neglected from this equation. This is called the Thomas-Fermi approximation. In this approximation, the energy functional is given by:

$$F = \int \mathrm{d}x \left(\sum_{i\in\{-1,0,1\}} (V - \mu_i)|\psi_i(\mathbf{r})|^2 + \frac{1}{2} \sum_{i,j\in\{-1,0,1\}} g_{i,j}|\psi_i(\mathbf{r})|^2|\psi_j(\mathbf{r})|^2 \right) \tag{27}$$

With which we have found the free energy equation for a spinor BEC.

3.2 Phase diagrams for three component spin-1 BEC

We will now proceed to find phase diagrams for the three component spinor BEC as has been illustrated by W. Ketterle et al [9]. In this case also the presence of an external magnetic field will be considered. Density profiles of these condensates will not be elaborated on, as the

purpose of this paragraph is just to give some general information. For this the previous free energy equations are not important, as we will only minimize the spin part of the free energy equation in a more general form. We will therefore introduce the Zeeman energy E_{ze} which can be written in the following form:

$$E_{ze} = E_+|\zeta_\uparrow|^2 + E_0|\zeta_0|^2 + E_\downarrow|\zeta_\downarrow|^2 \tag{28}$$

where $E_\uparrow$, E_0 and $E_\downarrow$ are the Zeeman energies for the $m_F = +1, 0, -1$ states and $\psi_i \equiv \sqrt{N}\zeta_i$ such that $|\zeta|^2 = 1$[10]. In these condensates, the total spin is conserved. As mentioned earlier, spinflip collisions, that is reactions of the form

$$|m_F = 0\rangle + |m_F = 0\rangle \leftrightarrow |m_F = +1\rangle + |m_F = -1\rangle \tag{29}$$

can occur at collision. The Zeeman energy difference E_{flip} can now easily be calculated

$$E_{flip} \equiv 2q = E_\uparrow + E_\downarrow - 2E_0. \tag{30}$$

Next to that we will define $2\widetilde{p} = E_\downarrow - E_\uparrow$.We can now rewrite the equation for q using the eigenvalue equations $F^2\,|f, m_f\rangle = f(f+1)\hbar^2\,|f, m_f\rangle$ and $F_z\,|f, m_f\rangle = m_f\hbar\,|f, m_f\rangle$ from which we derive the following matrix representation of these operators

$$F_z = \hbar\begin{pmatrix}1 & 0 & 0\\ 0 & 0 & 0\\ 0 & 0 & -1\end{pmatrix},\ F_z^2 = \hbar^2\begin{pmatrix}1 & 0 & 0\\ 0 & 0 & 0\\ 0 & 0 & 1\end{pmatrix},\ \mathbf{F} = (F_x, F_y, F_z) \tag{31}$$

In which

$$F_x = \frac{\hbar}{\sqrt{2}}\begin{pmatrix}1 & 0 & 0\\ 0 & 0 & 0\\ 0 & 0 & -1\end{pmatrix} \text{ and } F_y = \frac{\hbar}{\sqrt{2}}\begin{pmatrix}0 & -i & 0\\ i & 0 & -i\\ 0 & i & 0\end{pmatrix} \tag{32}$$

From which we can show that

$$2q = E_0 - \widetilde{p} < F_z > + q < F_z^2 > \tag{33}$$

We can now proceed and find the Free energy in our new notation. note that $< F >^2$ is equivalent to the interaction term up to a constant, that we now have an additional Zeeman energy in the equation. We will now use the same notation as Ketterle used in his paper and and instead of chemical potential use a Lagrange multiplier p_0 that conserves the total amount of spin. We then get a new equation for the free energy in Thomas-Fermi approximation given by

$$F = \int \mathrm{d}x\ N\left[V + \frac{c_0 N}{2} + \frac{c_2 N}{2} < \mathbf{F} >^2 + E_{ze} - p_0 < F_z >\right] \tag{34}$$

In which the constants are defined as $c_0 = 4\pi\hbar^2\overline{a}/m$, $c_2 = 4\pi\hbar^2\Delta a/m$ with $\overline{a} = (2a_2 + a_0)/3$ and $\Delta a = (a2 - a_0)/3$. Here, a_k is the scattering length for two atoms with total angular momentum $F = k$. It can be shown that this free energy differs from our old free energy equation 27 because it has a different Lagrange multiplier and an additional Zeeman energy. We can now take the spin dependent part from this equation which gives us

$$F_{Spin} = c < \mathbf{F} >^2 - p\hbar < \mathbf{F_z} > + q < \mathbf{F}_z^2 > \tag{35}$$

In which we defined that $p\hbar = \widetilde{p} + p_0$ and $c \equiv c_2 N/2$.

Minimization of F_{Spin} for parameters $|\zeta_\uparrow|^2$, $|\zeta_0|^2$, $|\zeta_\downarrow|^2$ now gives us us a phase diagram as a function of p, q and c. For c we can clearly separate three cases: The antiferromagnetic case $c > 0$, the case without interaction $c = 0$ and the antiferromagnetic case $c < 0$. We will now minimize this equation for the case with zero interaction and draw the phase diagram. Because the other cases can be derived in a similar fashion, we will only discuss their phase diagrams.

3.2.1 Case 1: zero interaction

In the case of zero interaction we have $c = 0$, which reduces the free energy equation to

$$F_{Spin} = -p\hbar < \mathbf{F_z} > +q < \mathbf{F}_z^2 > \tag{36}$$

substituting $< F_z >= \zeta^T F_z \zeta = \hbar(|\zeta_\uparrow|^2 - |\zeta_\downarrow|^2)$ and $< F_z^2 >= \zeta^T F_z \zeta = \hbar^2(|\zeta_\uparrow|^2 + |\zeta_\downarrow|^2)$, where $n_i = N|\psi_i|^2$, gives us the following equation.

$$F_{Spin}/\hbar^2 = -p\left(|\zeta_\uparrow|^2| - |\zeta_\downarrow|^2\right) + q\left(|\zeta_\uparrow|^2| + |\zeta_\downarrow|^2\right) = |\zeta_\uparrow|^2(q-p) + |\zeta_\downarrow|^2(q+p) \tag{37}$$

In which $|\zeta_\uparrow|^2 + |\zeta_0|^2 + |\zeta_\downarrow|^2 = 1$. Minimizing this equation for $|\zeta_\uparrow|^2$ and $|\zeta_\downarrow|^2$ can not simply be done by differentiating to these variables and putting them to zero, for differentiating to one of these variables yields a constant. Instead we have to consider all areas in the space $\{p, q\}$ and then minimize the free energy for these values, while also considering the constraint $|\zeta_\uparrow|^2 + |\zeta_0|^2 + |\zeta_\downarrow|^2 = 1$ together with the fact that the amount of particles cannot be a negative number. For example, take $q > 0$ together with $-q < p < q$. In this space, both $q - p > 0$ and $q + p > 0$ and thus the free energy is strictly bigger than 0. Therefore choosing $|\zeta_0|^2 = 1$ and thus $|\zeta_\uparrow|^2 = |\zeta_\downarrow|^2 = 0$ yields a free energy of 0 which is the minimum. In this area, there are therefore only spin 0 particles as is illustrated in part b of figure 5. Calculating the presence of the spin 0 phase for the whole domain yields

$$|\zeta_0(p,q)|^2 = \begin{cases} 1 & \text{if } q > 0 \text{ and } p \in (-q, q) \\ \text{undetermined} & \text{if } q \geq 0 \text{ and } |p| = q \\ 0 & \text{elsewhere} \end{cases} \tag{38}$$

When $|\zeta_0(p,q)|^2$ is undetermined, any value in $[0, 1]$ suffices as long as the appropriate constraints are considered. Considering all of these cases by hand is a long but simple process, and therefore it is convenient to use a software package to calculate these. Analogously, calculating the presence of other domains yields.

$$\begin{aligned} |\zeta_\uparrow(p,q)|^2 &= \begin{cases} 1 & \text{if } (q > 0 \text{ and } p > -q) \text{ or } (q \leq 0 \text{ and } p < 0) \\ \text{undetermined} & \text{if } (q < 0 \text{ and } p = 0) \text{ or } (q \geq 0 \text{ and } p = q) \\ 0 & \text{elsewhere} \end{cases} \\ |\zeta_\downarrow(p,q)|^2 &= \begin{cases} 1 & \text{if } (q > 0 \text{ and } p > q) \text{ or } (q \leq 0 \text{ and } p > 0) \\ \text{undetermined} & \text{if } (q < 0 \text{ and } p = 0) \text{ or } (q \geq 0 \text{ and } p = -q) \\ 0 & \text{elsewhere} \end{cases} \end{aligned} \tag{39}$$

Drawing these solutions is equivalent to phase diagram b of figure 5. Notice that all spin states are demixed.

3.2.2 Case 2 and 3: antiferromagnetic and ferromagnetic

In the antiferromagnetic case or equivalently when $c > 0$ we again need to minimize the free energy as defined in 35. This minimization is a similar but more elaborate process as in the case without interaction, and can easily be performed by a software package. This yields us with the results shown in diagram a of figure 5. Note that sodium is also antiferromagnetic.

Interestingly, there is now an area with spin-mixing between the $m_F = \pm 1$ states, but these states do not mix with the $m_F = 0$ state. We will again see similar behaviour for sodium in the next paragraphs.

Similarly the phase diagram for the ferromagnetic case can be derived, as is shown in phase diagram c of figure 5. In addition, we now see the gray area in which the spin 0 component can either mix with the spin 1 component for $p > 0$ or the spin -1 component for $p < 0$

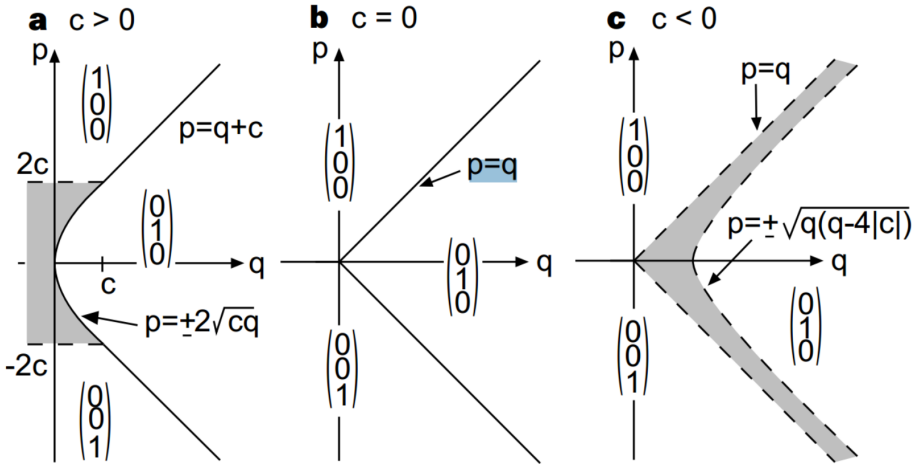

Figure 5 – Phase diagram as a function of linear Zeeman energy p and quadratic Zeeman energy q for different values of the constant c[10]. In a the antiferromagnetic case is shown. The gray area here indicates a spin mixture of the $m_F = \pm 1$ states. In b we chose zero interaction and finally in c, the ferromagnetic case, the gray area indicates a spin mixture between the $m_F = 0$ and the $m_F = 1$ state when $p > 0$ and the $m_F = 0$ and the $m_F = -1$ state when $p < 0$. This image was taken from [10].

3.3 Density profiles for two spin components

We will now examine the case in which we choose the chemical potentials in such as way that only particles with $m_F \in \{-1, 0\}$ are present in the condensate. It can be seen that there are in principle 4 different states for this freedom in spin. We can find places where only the $m_F = 0$ or the $m_F = -1$ state occur, mixtures of $m_F = 0$ and $m_F = -1$ and can find places for which there are no particles present at all. Denote $n_{-1}(x) = n_\downarrow(x)$. To find this profile we firstly rewrite equation 27 for this scenario and define $n_i(x) = |\psi_i(\mathbf{r})|^2$ such that

$$\mathrm{F} = \int \mathrm{d}x \left((V - \mu_0)\, n_0(x) + (V - \mu_\downarrow)\, n_\downarrow(x) + \frac{1}{2} g_{00} n_0^2(x) + \frac{1}{2} g_{\downarrow\downarrow} n_\downarrow^2(x) + g_{\downarrow 0} n_\downarrow(x) n_0(x) \right) \tag{40}$$

In this paragraph only the case in which $g_{00} g_{\downarrow\downarrow} - g_{\downarrow 0}^2 > 0$ is considered. The Hessian matrix of this free energy equation is given by

$$\begin{pmatrix} g_{00} & g_{\downarrow 0} \\ g_{\downarrow 0} & g_{\downarrow\downarrow} \end{pmatrix} \tag{41}$$

With eigenvalues $\lambda_\pm = \frac{1}{2}(g_{00} + g_{\downarrow\downarrow} \pm \sqrt{(g_{00} - g_{\downarrow\downarrow})^2 + 4 g_{\downarrow 0}})$. Both of these eigenvalues are strictly positive for $g_{00} g_{\downarrow\downarrow} - g_{\downarrow 0}^2 > 0$. Therefore, the hessian matrix is positive definite which means the extreme values are minima.

Minimizing the free energy as a function of n_0 and $n_\downarrow$ now amounts to taking the functional derivative of these variables and putting them equal to 0. However, the constraints that $n_0(x) > 0$ and $n_{-1}(x) > 0$ still holds for all x. Taking the functional derivatives with respect to $n_\downarrow(x)$ and $n_0(x)$ and putting them to 0 gives us the set of equations

$$\begin{aligned} V - \mu_0 + g_{00} n_0(x) + g_{\downarrow 0} n_\downarrow(x) &= 0 \\ V - \mu_\downarrow + g_{\downarrow\downarrow} n_\downarrow(x) + g_{\downarrow 0} n_0(x) &= 0 \end{aligned} \tag{42}$$

If we solve the set of equations in 42 we arrive at the following solutions

$$\begin{aligned} n_0(x) &= \frac{(g_{\downarrow 0} - g_{\downarrow\downarrow})V + g_{\downarrow\downarrow}\mu_0 - g_{\downarrow 0}\mu_\downarrow}{g_{00}g_{\downarrow\downarrow} - g_{\downarrow 0}^2} \\ n_\downarrow(x) &= \frac{(g_{\downarrow 0} - g_{00})V + g_{00}\mu_1 - g_{\downarrow 0}\mu_0}{g_{00}g_{\downarrow\downarrow} - g_{\downarrow 0}^2} \end{aligned} \tag{43}$$

Note that it is physically prohibited that $n_0(x) < 0$ or $n_{-1}(x) < 0$, so whenever we find a minimum for $n_0(x)$ or $n_\downarrow(x)$ smaller than 0, we choose it to be 0. We will choose the potential to be harmonic, which means that $V(x) = \kappa x^2$ for some constant κ. $n_0(x)$ now has the roots $x = \pm\frac{1}{\sqrt{\kappa}}\sqrt{\frac{g_{\downarrow 0}\mu_\downarrow - g_{\downarrow\downarrow}\mu_0}{g_{\downarrow 0} - g_{\downarrow\downarrow}}} \equiv \pm R_0$ and $n_\downarrow(x)$ has the roots $x = \pm\frac{1}{\sqrt{\kappa}}\sqrt{\frac{g_{00}\mu_\downarrow - g_{\downarrow 0}\mu_0}{g_{00} - g_{\downarrow 0}}} \equiv \pm R_\downarrow$. We must now factor in that in these formulas we did not factor in the fact that these populations can not be smaller than 0. we find that $R_0 \geq R_\downarrow$ if $\mu_\downarrow > \mu_0$. this means that for $|x| > R_\downarrow$ and $\mu_\downarrow > \mu_0$ we get $n_\downarrow = 0$ such that

$$n_0(x) = \begin{cases} \frac{(g_{\downarrow 0} - g_{\downarrow\downarrow})V + g_{\downarrow\downarrow}\mu_0 - g_{\downarrow 0}\mu_\downarrow}{g_{00}g_{\downarrow\downarrow} - g_{\downarrow 0}^2} & \text{if } x \in I_\downarrow \text{ and } \mu_\downarrow > \mu_0 \\ \frac{\mu_0 - V(x)}{g_{0,0}} & \text{if } x \in [-\sqrt{\frac{\mu_0}{\kappa}}, \sqrt{\frac{\mu_0}{\kappa}}] \setminus I_\downarrow \\ 0 & \text{elsewhere} \end{cases} \tag{44}$$

and the density profile of the $m_F = -1$ profile is given by:

$$n_\downarrow(x) = \begin{cases} n_\downarrow(x) = \frac{(g_{\downarrow 0} - g_{00})V + g_{00}\mu_1 - g_{\downarrow 0}\mu_0}{g_{00}g_{\downarrow\downarrow} - g_{\downarrow 0}^2} & \text{if } x \in I_\downarrow \\ 0 & \text{elsewhere} \end{cases} \tag{45}$$

Here we defined $I_\downarrow = [-R_\downarrow, R_\downarrow]$

In the case that $\mu_\downarrow \leq \mu_0$ we get the set of equations

$$\begin{aligned} n_0(x) &= \begin{cases} \frac{(g_{\downarrow 0} - g_{\downarrow\downarrow})V + g_{\downarrow\downarrow}\mu_0 - g_{\downarrow 0}\mu_\downarrow}{g_{00}g_{\downarrow\downarrow} - g_{\downarrow 0}^2} & \text{if } x \in I_0 \\ 0 & \text{elsewhere} \end{cases} \\ n_\downarrow(x) &= \begin{cases} \frac{(g_{\downarrow 0} - g_{00})V + g_{00}\mu_1 - g_{\downarrow 0}\mu_0}{g_{00}g_{\downarrow\downarrow} - g_{\downarrow 0}^2} & \text{if } x \in I_0 \\ \frac{\mu_1 - V}{g_{\downarrow\downarrow}} & \text{if } x \in [-\sqrt{\frac{\mu_1}{\kappa}}, \sqrt{\frac{\mu_1}{\kappa}}] \setminus I_0 \\ 0 & \text{elsewhere} \end{cases} \end{aligned} \tag{46}$$

In which we defined $I_0 = [-R_0, R_0]$ For certain choices of g_{ij} graphs of this function have been drawn in figure 6.

We can now proceed by drawing phase diagrams for a certain choice of g_{00}, $g_{\downarrow 0}$ and $g_{\downarrow\downarrow}$. Let us for instance choose $g_{00} = g_{\downarrow\downarrow} > g_{\downarrow 0} > 0$ which satisfies the required condition $g_{00}g_{\downarrow\downarrow} - g_{\downarrow 0}^2 > 0$. In this case we see that $(g_{\downarrow 0} - g_{\downarrow\downarrow})V = (g_{\downarrow 0} - g_{00})V$ such that $n_0(x)$ and $n_\downarrow(x)$ have the same derivative when both are nonzero and we note that we need $\mu_0 > \frac{g_{\downarrow 0}}{g_{\downarrow\downarrow}}\mu_\downarrow$ in order for $n_0(x)$ to be nonzero and we need $\mu_\downarrow > \frac{g_{\downarrow 0}}{g_{00}}\mu_0 = \frac{g_{\downarrow 0}}{g_{\downarrow\downarrow}}\mu_0$ for $\mu_\downarrow$ to be nonzero. So for both of them to be nonzero we need $\mu_0 \in (\frac{g_{\downarrow 0}}{g_{\downarrow\downarrow}}\mu_\downarrow, \frac{g_{\downarrow\downarrow}}{g_{\downarrow 0}}\mu_\downarrow)$. This results in the phase-diagram given in figure 7 The final thing we will do is calculate the amount of particles in the trap N. This is simply found by integrating the functions found in figure 6. We will only derive this for the case that $g_{00} > g_{\downarrow\downarrow} = g_{\downarrow 0}$. Then we find that

$$\begin{cases} n_{-1} = \frac{8\sqrt{\kappa}\left(\frac{g_{-1,0}\mu_0 - g_{0,0}\mu_1}{g_{-1,0} - g_{0,0}}\right)}{3g_{-1,0}} \\ n_0 = \frac{4}{3\sqrt{2}\kappa g_{0,0}(g_{1,0} - g_{0,0})}\left(g_{-1,0}\mu_0\left(\sqrt{\mu_0} - \sqrt{\frac{g_{-1,0}\mu_0 - g_{0,0}\mu_1}{g_{-1,0} - g_{0,0}}}\right) + g_{0,0}\left(\mu_0^{3/2} - \mu_1\sqrt{\frac{g_{-1,0}\mu_0 - g_{0,0}\mu_1}{g_{-1,0} - g_{0,0}}}\right)\right) \end{cases} \tag{47}$$

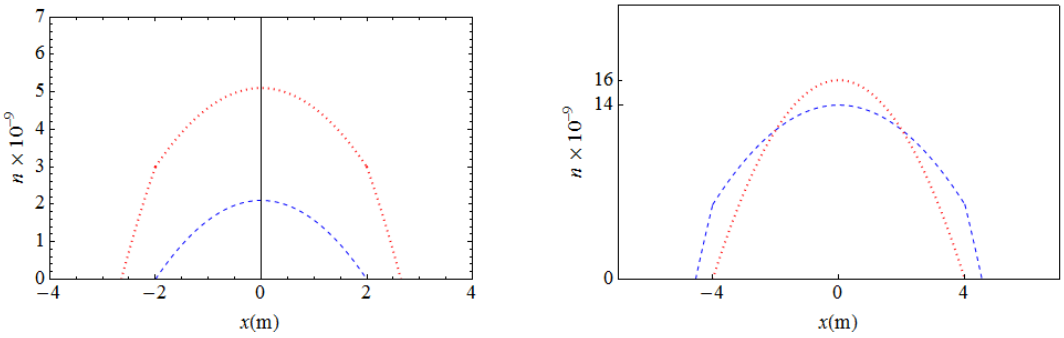

Figure 6 – Plot of amount of particles as a function of the position x in the case that $g_{00} = g_{\downarrow\downarrow} > g_{\downarrow 0} > 0$, all in units of $\mathrm{m}^5\mathrm{kg/s}^2$. the dotted line(red) represents the amount of particles in the $m_F = 0$ phase and the striped line the amount of particles with $m_F = -1$. Specifically in the left figure, $g_{\downarrow\downarrow} = g_{00} = 1 > g_{\downarrow 0} = 0.9$, $\mu_0 = 7$, $\mu_\downarrow = 6.7$ and $\kappa = 1$. In the right figure we $g_{00} > g_{\downarrow\downarrow}$ and $\mu_0 > \mu_\downarrow$.

3.4 Density profiles with saddle point for two spin components

In the previous paragraph, density profiles were calculated for the case that $g_{00}g_{\downarrow\downarrow} - g_{\downarrow 0}^2 > 0$. In this paragraph, we will assume that $g_{00}g_{\downarrow\downarrow} - g_{\downarrow 0}^2 < 0$. As a consequence, the Hessian matrix calculated in 41 now has one positive and one negative eigenvalue. Therefore, the extremum found by using equation 42 gives a saddle point instead of a minimum and any minima must be on the boundaries of the space spanned by $\{n_0(x), n_{-1}(x)\}$. If n_0 or n_{-1} goes to infinity, the free energy according to equation 40 will also go to infinity when we choose the potential to be $V = \kappa x^2$ with $\kappa > 0$. We can therefore reduce the free energy equation to The energy goes to infinity for either n_0 or n_{-1} goes to infinity, so we require for every x that either $n_0(x) = 0$ or $n_{-1}(x) = 0$. Therefore, the energy equation reduces to:

$$F(x) = (V - \mu_0)\, n_0(x) + (V - \mu_\downarrow)\, n_\downarrow(x) + \frac{1}{2} g_{00} n_0^2(x) + \frac{1}{2} g_{\downarrow\downarrow} n_\downarrow^2(x) \tag{48}$$

and we require that for every x that either $n_0(x) = 0$ or $n_{-1}(x) = 0$ such that we are still on the boundary of the space. Therefore we can rewrite this equation and seperate two cases

$$F(x) = \begin{cases} (V - \mu_0)\, n_0(x) + \frac{1}{2} g_{00} n_0^2(x) & \text{if } n_0 > 0 \\ (V - \mu_\downarrow)\, n_\downarrow(x) + \frac{1}{2} g_{\downarrow\downarrow} n_\downarrow^2(x) & \text{if } n_\downarrow > 0 \\ 0 & \text{elsewhere} \end{cases} \tag{49}$$

This means that there will never be a mixture of the $m_F = -1$ and $m_F = 0$ states. We will now proceed by calculating the density profiles n_0 and $n_\downarrow$ by minimizing the free energy equation. The Hessian matrix of the new free energy equation is then given by

$$\begin{pmatrix} g_{00} & 0 \\ 0 & g_{\downarrow\downarrow} \end{pmatrix} \tag{50}$$

Which has the two positive eigenvalues g_{00} and $g_{\downarrow\downarrow}$ such that it is a positive definite matrix. We know from mathematical theory that the extreme values of a positive definite matrix are minima, so we can find the minimum of the free energy by taking the partial derivative of $F(n_0, n_\downarrow)$ in n_0 and $n_\downarrow$ and putting them to 0. This gives us a set of equations:

$$\begin{aligned} (V - \mu_0) + g_{00} n_0(x) &= 0 \text{ if } n_0 > 0 \\ (V - \mu_\downarrow) + g_{\downarrow\downarrow} n_\downarrow(x) &= 0 \text{ if } n_\downarrow > 0 \end{aligned} \tag{51}$$

They are easily solved for either $n_0(x) = \frac{\mu_0 - V(x)}{g_{00}}$ and $n_\downarrow(x) = 0$ with $F(x) = -\frac{(\mu_0 - V(x))^2}{2g_{00}} \equiv F_0(x)$ or $n_0(x) = 0$ and $n_\downarrow(x) = \frac{\mu_\downarrow - V(x)}{g_{\downarrow\downarrow}}$ with $F(x) = -\frac{(\mu_\downarrow - V(x))^2}{2g_{\downarrow\downarrow}} \equiv F_\downarrow(x)$. Note that $n_0(x)$

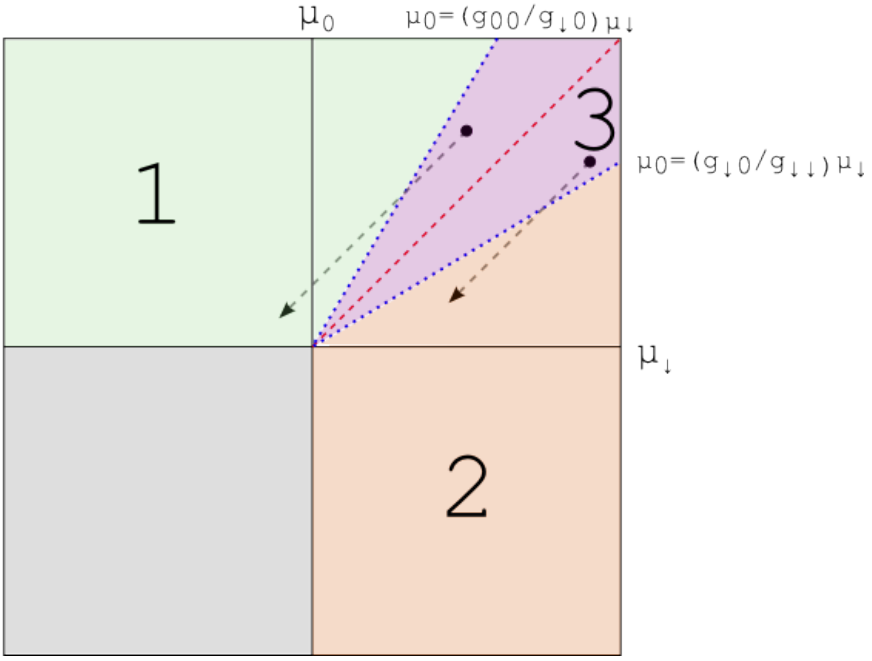

Figure 7 – Phase diagram at $x = 0$ in the case that $g_{00} = g_{\downarrow\downarrow} > g_{\downarrow 0} > 0$ and with the constraint that there are only $m_F = -1$ and $m_F = 0$ particles. Here μ_0 is chosen on the vertical axis and $\mu_\downarrow$ is chosen on the horizontal axis. Area 1 symbolizes the area in which there are only particles in the $m_F = 0$ state, area 2 symbolizes the area in which all particles are in the $m_F = -1$ state and in area 3 we find a mixture of both states. When $x > 0$, samples with starting value of $\{\mu_\downarrow, \mu_0\}$ will move in the direction of the dashed arrows visible in the diagram. This symbolizes the phase change as a result of the harmonic potential. Note that the arrows are parallel to the line $\mu_0 = \mu_\downarrow$ such that it is possible to find a mixture of both states around $x = 0$ and $m_F = -1$ on the outsides if $\mu_\downarrow > \mu_0$, or $m_F = 0$ on the outsides if $\mu_\downarrow < \mu_0$.

and $n_\downarrow(x)$ should always be bigger than or equal to 0, as before. For every x we can now choose the function in 49 that minimizes the free energy, i.e. we can take the minimum of $F_0(x)$, $F_\downarrow(x)$ and 0. We again choose $V = \kappa x^2$ to be the harmonic potential, $\mu_0(x) = \mu_0 - V(x)$ and $\mu_\downarrow(x) = \mu_\downarrow - V(x)$. With this we can rewrite the minimum of the free energy equation as

$$F(x) = \begin{cases} F_0(x) = -\frac{\mu_0(x)^2}{2g_{00}} & \text{if } n_0 > 0 \text{ and } n_\downarrow = 0 \\ F_\downarrow(x) = -\frac{\mu_\downarrow(x)^2}{2g_{\downarrow\downarrow}} & \text{if } n_0 = 0 \text{ and } n_\downarrow > 0 \\ 0 & \text{elsewhere} \end{cases} \tag{52}$$

There are now three cases to consider.

1. We get the $m_F = 0$ phase at a point x_0 if $\min[F_0(x_0), F_\downarrow(x_0), 0] = F_0(x_0)$ and $n_0(x_0) = \frac{\mu_0(x_0)}{g_{00}} > 0$ or $\mu_0(x_0) > 0$. We therefore require firstly that $F_0(x_0) < 0$ which is true for all $\mu_0(x_0)$. Secondly, it is required that $F_0(x) < F_\downarrow(x)$ or we need $n_\downarrow \leq \frac{\mu_\downarrow(x)}{g_{\downarrow\downarrow}}$. Therefore we either need that $\mu_0(x) > \pm\sqrt{\frac{g_{00}}{g_{\downarrow\downarrow}}}\mu_\downarrow(x)$ or $\mu_\downarrow \leq 0$. Combining this gives that we need

either $\mu_0(x) > \sqrt{\frac{g_{00}}{g_{\downarrow\downarrow}}}\mu_\downarrow(x)$ if $\mu_\downarrow(x) > 0$ or $\mu_0(x) > 0$ and $\mu_\downarrow(x) \leq 0$.

2. Analogously, we find the $m_F = -1$ phase at a point x_0 if $\min[F_0(x_0), F_\downarrow(x_0), 0] = F_\downarrow(x_0)$ and $n_\downarrow(x_0) = \frac{\mu_\downarrow(x_0)}{g_{\downarrow\downarrow}} > 0$ or $\mu_\downarrow(x_0) > 0$. We therefore require firstly that $F_\downarrow(x_0) < 0$ which is true for all $\mu_\downarrow(x_0)$. Secondly, it is required that $F_\downarrow(x) < F_0(x)$ or we need $n_0 \leq \frac{\mu_0(x)}{g_{00}}$. Therefore we either need that $\mu_\downarrow(x) > \pm\sqrt{\frac{g_{\downarrow\downarrow}}{g_{00}}}\mu_0(x)$ or $\mu_0 \leq 0$. Combining this gives that we need either $\mu_\downarrow(x) > \sqrt{\frac{g_{\downarrow\downarrow}}{g_{00}}}\mu_0(x)$ if $\mu_0(x) > 0$ or $\mu_\downarrow(x) > 0$ and $\mu_0(x) \leq 0$.

3. We find a vacuum for both $\mu_0 < 0$ and $\mu_\downarrow < 0$.

This results are shown in the form of a phase diagram in figure 8. Now we calculate explicitly

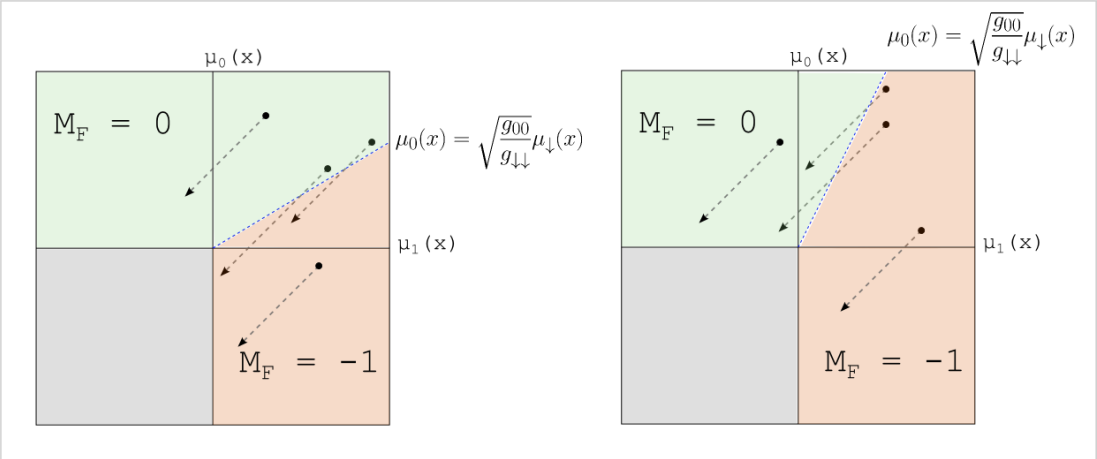

Figure 8 – Phase diagram of spinor BEC with $F = 1$ and $g_{00}g_{\downarrow\downarrow} - g_{\downarrow 0}^2 < 0$. Because $\mu_0(x)$ and $\mu_\downarrow(x)$ have the same derivative in x, once starting values μ_0 and $\mu_\downarrow$ have been chosen, the point moves down over the line $\mu_0(x) = \mu_\downarrow(x)$ as $V(x)$ increases. This makes it possible to change phase as $|x|$ increases. In the left diagram we chose $g_{\downarrow\downarrow} > g_{00}$ such that the $m_F = 0$ state turns into the $m_F = -1$ state for $0 < \sqrt{\frac{g_{00}}{g_{\downarrow\downarrow}}}\mu_\downarrow < \mu_0(x) < \mu_\downarrow(x)$. Note that the converse, i.e. the $m_F = -1$ state turns into the $m_F = 0$ state is not possible for the left diagram, because $V(x)$ can only increase. In the right diagram $g_{\downarrow\downarrow} < g_{00}$ was chosen such that the $m_F = -1$ state turns into the $m_F = 0$ state for $0 < \mu_\downarrow(x_0) < \mu_0(x_0) < \sqrt{\frac{g_{00}}{g_{\downarrow\downarrow}}}\mu_\downarrow(x_0)$ for some $x > x_0$. sketch of phases with the dashed line a possibility of transition for different V

the $n_0(x)$ and $n_{-1}(x)$ density profiles for different cases for a harmonic potential for the case $g_{00} < g_{\downarrow 0} = g_{\downarrow\downarrow}$:

1. Suppose that $0 < \sqrt{\frac{g_{00}}{g_{\downarrow\downarrow}}}\mu_\downarrow < \mu_0 < \mu_\downarrow$ such that we find the $m_F = 0$ phase in $x = 0$. As can be seen from the phase diagram, we can then find an x such that the $m_F = -1$ state is found. Firstly, define the following constants as

$$a \equiv \sqrt{\frac{1}{\kappa}\frac{\mu_0 - \sqrt{\frac{g_{00}}{g_{\downarrow\downarrow}}}\mu_\downarrow}{1 - \sqrt{\frac{g_{00}}{g_{\downarrow\downarrow}}}}} \qquad b \equiv \sqrt{\frac{\mu_\downarrow}{\kappa}} \tag{53}$$

We can calculate that $F_0(x) = F_\downarrow(x)$ for $x = \pm a$. Therefore, we find the $m_F = 0$, state for $x \in [-a, a]$. For $|x| > |a|$ we find the $m_F = -1$ state as long as $F_\downarrow(x) = -\frac{\mu_\downarrow(x)^2}{2g_{\downarrow\downarrow}} < 0$

. This is true for $x \in (-b,-a) \cup (a,b)$. For other x, i.e. $|x| > b$, we find a vacuum. It is now a simple but tedious exercise to calculate n_0 and $n_\downarrow$ by integrating over these areas.

2. Suppose that $\mu_0 > \mu_\downarrow$ and $\mu_0 > 0$. Then $F_0 < F_\downarrow$ for all x. Next to that we find that $n_0(x) = \frac{\mu_0 - \kappa x^2}{g_{00}} > 0$ for $x \in (-\sqrt{\frac{\mu_0}{\kappa}}, \sqrt{\frac{\mu_0}{\kappa}})$. This means that we find the $m_F = 0$ phase for $x \in (-\frac{\mu_0}{\kappa}, \frac{\mu_0}{\kappa})$ and a vacuum for all other x. Furthermore, we can find the amount of particles by integrating:

$$n_0 = \int_{-\frac{\mu_0}{\kappa}}^{\frac{\mu_0}{\kappa}} \mathrm{d}x \frac{\mu_0 - \kappa x^2}{g_{00}} = \frac{2}{3} \frac{\mu_0^{3/2}}{g_{00}\sqrt{\kappa}} \qquad (54)$$
$$n_\downarrow = 0$$

3. Finally, suppose that $0 < \mu_0 < \sqrt{\frac{g_{-1,0}}{g_{0,0}}}\mu_{-1}$ then we find the $n_\downarrow$ phase for $x \in [-b, b]$

a summary of these results can be found in figure 9.

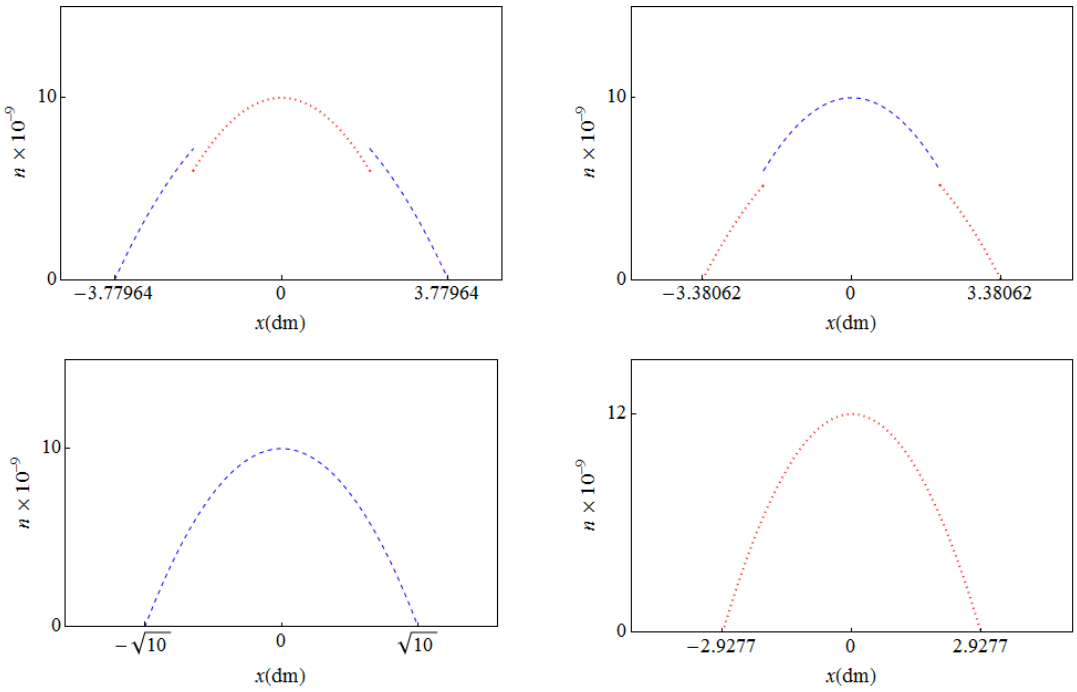

Figure 9 – Plots of density profiles $n_0(x)$ which is represented as a dotted red line and $n_\downarrow(x)$ represented as a dashed blue line. In the top left figure, situation 1 is shown: we find the $m_F = 0$ phase close to $x = 0$ and then suddenly the phase changes to $m_F = -1$. Note the discontinuity at the interface of the $m_F = 0$ and $m_F = -1$ phases. On the bottom left case 3 is considered, with only the $m_F = -1$ phase occurring. On the bottom right only the $m_F = 0$ phase is present. We can see that at the roots of both the bottom left and bottom right plots there is no discontinuity, but they are not differentiable in the points shown in the plot. The top right plot shows a fourth situation in which $g_{\downarrow\downarrow} < g_{00}$ such that the $m_F = -1$ phase occurs close to 0 with the $m_F = -1$ phase on the outside.

4 Approximations of the interface.

In the previous chapter we derived equations and phase diagrams for the density profiles of different spin states. The Thomas-Fermi approximation was used, which assumes that the kinetic part of the Gross-Pitaevskii equation is much smaller than the interaction part and can thus be neglected. As a consequence of this, the functions $n_0(x)$ and $n_\downarrow(x)$ could get infinitely steep derivatives in x at their interfaces. Therefore, the Thomas-Fermi approximation is not valid in this neighborhood and a new method of approximation should be found. In this chapter, we will try approximating the solution of the GPE by using the results found in chapter 3. Subsequently these results will be refined using numerical methods.

4.1 Adding the kinetic energy term

Instead of using the free Thomas-Fermi approximation, we could try minimizing the free-energy equation introduced in equation 22 and adapted for the case of a multi component system in equation 27. We then get the following equation:

$$F(\psi_0(x),\psi_\downarrow(x)) = \int \mathrm{d}x \left[\frac{\hbar^2}{2m} \left(\frac{\partial \psi_0(x)}{\partial x}^2 + \frac{\partial \psi_\downarrow(x)}{\partial x}^2 \right) + (V-\mu_0)\, n_0(x) + (V-\mu_\downarrow)\, n_\downarrow(x) \right. \\ \left. + \frac{1}{2} g_{00} n_0^2(x) + \frac{1}{2} g_{\downarrow\downarrow} n_\downarrow^2(x) + g_{\downarrow 0} n_\downarrow(x) n_0(x) \right] \tag{55}$$

We now want to focus on the interface between the $m_F = 0$ phase and the $m_F = -1$ phase. To do this, we introduce a potential together with two chemical potentials such that on the negative side of the x axis we find the $m_F = -1$ phase and on the positive side of the x axis we find the $m_F = 0$ phase in Thomas-Fermi approximation.For this, we choose $V(x) = -\epsilon x$ with ϵ arbitrarily small and we choose $\mu_0 = \sqrt{\frac{g_{00}}{g_{\downarrow\downarrow}}}\mu_\downarrow > 0$. This is basically a Taylor approximation on the harmonic potential. As long as we are close to the interface, this approximation is valid. Since we are only interested in the behaviour around the interface there is a valid reason to use this potential. We can take $V = 0$ as a simplification and remind ourselves that we are looking for a solution with $m_F = -1$ if $x < 0$ and $m_F = -1$ if $x > 0$. This gives us

$$F(\psi_0(x),\psi_\downarrow(x)) = \int \mathrm{d}x \left[\frac{\hbar^2}{2m} \left(\frac{\partial \psi_0(x)}{\partial x}^2 + \frac{\partial \psi_\downarrow(x)}{\partial x}^2 \right) - \sqrt{\frac{g_0}{g_1}}\mu_1 |\psi_0(x)|^2 - \mu_\downarrow |\psi_\downarrow(x)|^2 \right. \\ \left. + \frac{1}{2} g_{00} |\psi_0(x)|^4 + \frac{1}{2} g_{\downarrow\downarrow} |\psi_\downarrow(x)|^4 + g_{\downarrow 0} |\psi_\downarrow(x)|^2 |\psi_0(x)|^2 \right] \tag{56}$$

We now want to minimize this free energy equation. In paragraph 3.4 of the previous chapter we found that $n_0(x) = \frac{\mu_0 - V(x)}{g_0}$ and $n_1(x) = \frac{\mu_1 - V(x)}{g_1}$ in Thomas-Fermi approximation. Choosing $V(x) = 0$ now gives us the solutions $\psi_0(x) = \sqrt{\frac{\mu_0}{g_0}}$ and $\psi_1(x) = \sqrt{\frac{\mu_1}{g_1}}$. Defining $c \equiv \sqrt{\frac{g_{\downarrow\downarrow}\mu_0}{g_{00}\mu_\downarrow}}$, we note that $\psi_0(x) = c\psi_\downarrow(x)$. However, for $V(x) = -\epsilon x$ we find that in Thomas-Fermi approximation

$$\psi_0(x) = \begin{cases} 0 \text{ if } x < 0 \\ \sqrt{\frac{\mu_0}{g_{00}}} \text{ if } x > 0 \end{cases} \quad \text{and } \psi_\downarrow(x) = \begin{cases} \sqrt{\frac{\mu_\downarrow}{g_{\downarrow\downarrow}}} \text{ if } x < 0 \\ 0 \text{ if } x > 0 \end{cases} \tag{57}$$

Therefore, the function $\psi_0(x) + c\psi_1(x) = \psi_0 + c\psi_1$ is a continuous and constant function with derivative 0 in Thomas-Fermi approximation. Also note that $\psi_\downarrow(x)/2 - \psi_0(x)/2c$ is an anti-symmetric function because of the minus sign. This inspires us to define the following transformation functions

$$\begin{aligned} \psi_+(x) &= \psi_0(x) + c\psi_\downarrow(x) \\ \psi_-(x) &= -\frac{\psi_0(x)}{2c} + \frac{\psi_\downarrow(x)}{2} \end{aligned} \tag{58}$$

With $c = \sqrt{\frac{g_{\downarrow\downarrow}\mu_0}{g_{00}\mu_\downarrow}}$. Note that $\psi_+(x)$ is equal to the constant value $\sqrt{\frac{\mu_0}{g_{00}}}$ and using that $\mu_0 = \sqrt{\frac{g_{00}}{g_{\downarrow\downarrow}}}\mu_\downarrow > 0$ we can rewrite that $c = \left(\frac{g_{\downarrow\downarrow}}{g_{00}}\right)^{\frac{1}{4}}$. Plots of $\psi_0(x)$ together with $\psi_\downarrow(x)$ and $\psi_+(x)$ together with $\psi_-(x)$ can be found in figure 10.

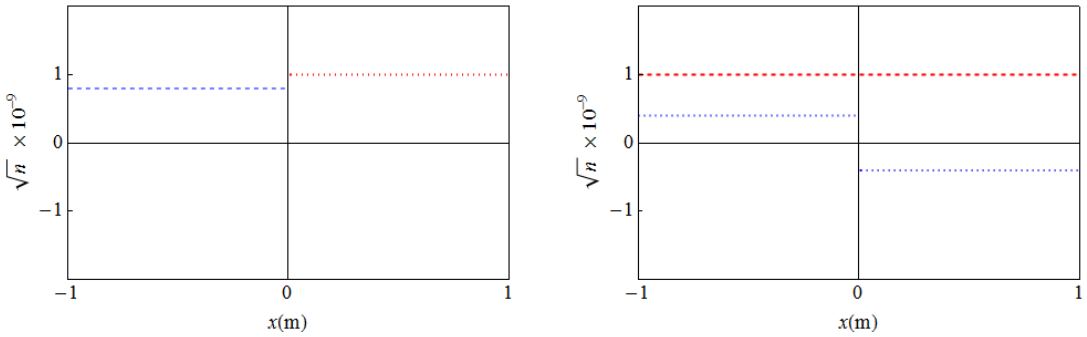

Figure 10 – In the left figure, a plot of the function $\psi_\downarrow(x)$ is shown as a dashed blue line and a plot of the function $\psi_0(x)$ is shown as a red dotted line. discontinuities are clearly visible for both phases. In the right figure, a plot of the function $\psi_+(x)$ is shown as a dashed red line and a plot of the function $\psi_-(x)$ is shown as a dotted blue line. In this figure, it can be seen that $\psi_+(x)$ is now a continuous and differentiable function.

The Jacobian matrix of this transformation can be written as

$$\begin{pmatrix} 1 & c \\ -\frac{1}{2c} & \frac{1}{2} \end{pmatrix} \tag{59}$$

Which has determinant 1. We can solve this set of equations for $\psi_0(x)$ and $\psi_\downarrow(x)$ which gives us the set of equations:

$$\begin{aligned} \psi_0 &= \psi_+/2 - c\psi_- \\ \psi_\downarrow &= \psi_+/2c + \psi_- \end{aligned} \tag{60}$$

We will now try to solve the free energy equation without the Thomas-Fermi approximation. From now on, we will consider $\psi_+(x)$ to be completely constant such that $\frac{\partial\psi_+(x)}{\partial x} = 0$, but we will take into account that $\frac{\partial\psi_-(x)}{\partial x} \neq 0$. First of all, defining that $P = (1+c^2)\frac{\hbar^2}{2m}$, we get that

$$\frac{\hbar^2}{2m}\left(\frac{\partial\psi_0(x)}{\partial x}^2 + \frac{\partial\psi_1(x)}{\partial x}^2\right) = P\left(\frac{\partial\psi_-(x)}{\partial x}\right)^2 \tag{61}$$

We use the fact that $\psi_+(x) = \sqrt{\frac{\mu_0}{g_{00}}}$ and continue substituting the equations for $\psi_0(x)$ and $\psi_\downarrow(x)$ into the free energy equation such that we get the following equation after some simple yet tedious algebra.

$$F(x) = \int \mathrm{d}x \left[P\left(\frac{\partial\psi_-(x)}{\partial x}\right)^2 + A\psi_-^4 - B\psi_-(x)^2 - C\right] \tag{62}$$

Here the constants A, B and C are strictly bigger than 0 and are given by

$$\begin{aligned} A &= g_{\downarrow\downarrow}\left(1 + \sqrt{\frac{g_{\downarrow\downarrow}}{g_{00}}}\right) \\ B &= \frac{\mu_0}{2}\left(\frac{g_{\downarrow\downarrow}}{g_{00}} + \sqrt{\frac{g_{\downarrow\downarrow}}{g_{00}}}\right) \\ C &= \frac{\mu_0^2}{16 g_{00}}\left(7 - \sqrt{\frac{g_{\downarrow\downarrow}}{g_{00}}}\right) \end{aligned} \tag{63}$$

What we now have is the simplified form of the free energy as a function of ψ_-. We now want to minimize the free energy to find the optimal value for $\psi_-(x)$ Since this is a functional, we can take the functional derivative of F. Write $F(x) = E(x, \psi_-(x), \frac{d\psi_-(x)}{dx}) := F(\epsilon)$. Then it follows that

$$\frac{\delta E}{\delta \psi_-} = \frac{\partial E(\epsilon)}{\partial \psi} - \frac{\partial}{\partial x}\frac{\partial E(\epsilon)}{\partial \frac{\partial \psi}{\partial x}} = -2P\frac{\partial^2 \psi_-}{\partial x^2} + 4A\psi_-^3 - 2B\psi_- \tag{64}$$

Now we equal this to 0 to find the minimum energy for ψ_- Notice that this is equivalent to putting.

$$P\left(\frac{\partial \psi_-}{\partial x}\right)^2 = \left(A\psi_-^4 - B\psi_-^2 + C_1\right) \tag{65}$$

This is a nonlinear differential equation for which we will find analytical solutions in the next paragraph.

4.2 Boundary conditions and solutions

In the previous paragraph we have found a non-linear differential equation for $\psi_-(x)$. we are now going to solve this equation, starting by determining the appropriate boundary conditions. As we get further from the interface, the solutions will be more like the solutions found using the Thomas-Fermi approximation. We therefore know that in $x = -\infty$, $\psi_- = {}^{\psi_1}/_2 = \frac{1}{2}\sqrt{\frac{\mu_1}{g_1}} = \sqrt{\frac{B}{2A}}$. Secondly, in the limit that x goes to ∞, the derivative of ψ_- goes to 0 which forms the second boundary condition. Summarizing this we have the following boundary conditions:

$$\begin{aligned} \psi_-(\infty) &= \sqrt{\frac{B}{2A}} \\ \frac{\partial \psi_-}{\partial x}(\infty) &= 0 \end{aligned} \tag{66}$$

To solve the differential equation as defined in 65, we will make our variable dimensionless. This inspires us to define the transformations $x = \sqrt{\frac{P}{B}}\tilde{x}$ and $\psi_- = \sqrt{\frac{B}{2A}}\tilde{\psi}_-$. Substituting this into equation 65 and rewriting it gives:

$$\frac{B^2}{2A}\left(\frac{\partial \tilde{\psi}_-}{\partial \tilde{x}}\right)^2 = \frac{B^2}{4A}(\tilde{\psi}_-^2 - 1)^2 - \frac{B^2}{4A} + C_1 \tag{67}$$

We know from the boundary conditions that $\psi_-(\infty) = \sqrt{\frac{B}{2A}}$ such that $\tilde{\psi}_-(\infty) = 1$ as well as $\frac{\partial \psi_-}{\partial x}(\infty) = \frac{\partial \tilde{\psi}_-}{\partial \tilde{x}}(\infty) = 0$. From this we conclude that $C_1 = \frac{B^2}{4A}$ elimination both the constant terms $-\frac{B^2}{4A}$ and C_1. Taking the square root, this leaves us with the equation

$$\sqrt{2}\frac{\partial \tilde{\psi}_-}{\partial \tilde{x}} = \tilde{\psi}_-^2 - 1 \tag{68}$$

This can easily be solved, providing us with the solution $\tilde{\psi}_- = -\tanh\frac{\tilde{x}}{\sqrt{2}}$. When we transform the variable $\tilde{x}$ and $\tilde{\psi}_-$ back to their original counterparts, we arrived at the final solution for $\psi_-(x$.

$$\psi_-(x) = -\sqrt{\frac{B}{2A}}\tanh\sqrt{\frac{B}{2P}}x \tag{69}$$

As we expected, this solution satisfies the boundary conditions, making it an anti-symmetric continuous and differentiable function. However, we originally set out to find solutions for $\psi_0(x)$ and $\psi_\downarrow(x)$. If we now apply the transformation in equation 58 , we arrive at the solutions for these wave functions.

$$\begin{aligned}\psi_0(x) &= \frac{1}{2}\frac{\mu_0}{g_{00}}\left(1+\tanh(\xi x)\right)\\ \psi_\downarrow(x) &= \frac{1}{2}\frac{\mu_\downarrow}{g_{\downarrow\downarrow}}\left(1-\tanh(\xi x)\right)\\ \xi &= \sqrt{\frac{m\mu_\downarrow}{2\hbar^2}}\end{aligned} \tag{70}$$

Plots of $\psi_+(x)$ together with $\psi_-(x)$ and $\psi_0(x)$ together with $\psi_\downarrow(x)$ are shown in figure 11.

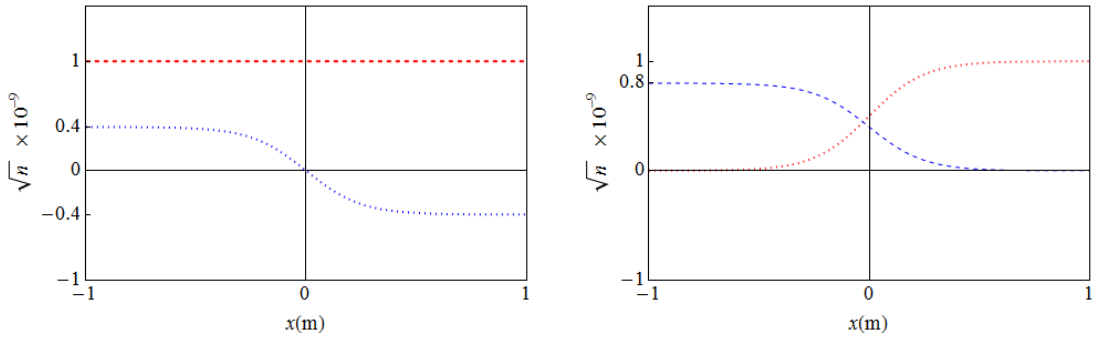

Figure 11 – In the left figure, a plot of the function $\psi_+(x)$ is shown as a dashed red line and a plot of the function $\psi_-(x)$ is shown as a dotted blue line. Both $\psi_+(x)$ and $\psi_-(x)$ are now continuous and differentiable functions. In the right figure, a plot of the function $\psi_\downarrow(x)$ is shown as a dashed blue line and a plot of the function $\psi_0(x)$ is shown as a red dotted line. There are no longer any discontinuities and both functions are differentiable.

The functions we found form a better approximation of the interface than in the case of the Thomas-Fermi approximation. There are however ways to improve this approximation by finding a better approximation of $\psi_+(x)$. We see that there is an area in which the $m_F = 0$ and $m_F = -1$ states mix. The factor ξ in the solutions for $\psi_0(x)$ and $\psi_\downarrow(x)$ gives us some information about the with of the interface. If this interface is relatively big compared to the size of the spin domains, then the Thomas-Fermi approximation is not valid.

4.3 Numerical enhancements

In this final paragraph we will show how to improve the approximation made in last paragraph by using numerical methods. We have found a better description of the interface, but earlier we assumed that $\psi_+(x)$ is completely constant. This assumption may indeed be correct in first approximation, but in order to improve our model of the interface we will now assume that $\psi_+(x)$ is not constant and we assume that $\psi_-(x) = -\sqrt{\frac{B}{2A}}\tanh\sqrt{\frac{B}{2P}}x$ is still the correct solution. We are going to substitute this solution into the free energy equation 56 and then minimize it as a function of $\psi_+(x)$. Before we continue, we are firstly going to define some constants and functions that will be convenient later in this paragraph

$$\begin{aligned}g_{eff} &= \frac{1}{4}(g_{00}+\sqrt{g_{00}g_{\downarrow\downarrow}})\\ V^*(x) &= \left[3\sqrt{g_{00}g_{\downarrow\downarrow}}-g_{\downarrow\downarrow}\right]\psi_-(x)^2-\mu_0\\ J(x) &= \frac{\hbar^2}{2m}\left(\frac{1}{c}-c\right)\frac{\partial^2\psi_-(x)}{\partial x^2}\\ R &= \frac{1}{2}\left(1+\frac{1}{c^2}\right)\frac{\hbar^2}{2m}\end{aligned} \tag{71}$$

Let us now rewrite the free energy equation. After some tedious algebra in which earlier mentioned algebraic identities for c en $\mu_\downarrow$ are used substituted, we arrive at the following equation for the free energy.

$$F(\psi_+(x)) = \int \mathrm{d}x \left[\frac{R}{2} \left(\frac{\partial \psi_+(x)}{\partial x} \right)^2 + \frac{\hbar^2}{2m} \left(\frac{1}{c} - c \right) \left(\frac{\partial \psi_-(x)}{\partial x} \right) \left(\frac{\partial \psi_+(x)}{\partial x} \right) + \frac{g_{eff}}{4} \psi_+^4(x) + \frac{V^*(x)}{2} \psi_+^2(x) + T\left(\psi_-(x)\right) \right] \tag{72}$$

In which $T\left(\psi_-(x)\right)$ is some kind of function that does not depend on $\psi_+(x)$. As in previous paragraph, the free energy can now be minimized by taking the functional derivative in $\psi_+(x)$ and putting it equal to zero. This gives us the equation:

$$\left\{ R \frac{\partial^2}{\partial x^2} + V^*(x) + g_{eff} (\psi_+(x))^2 \right\} \psi_+(x) = J(x) \tag{73}$$

This equation is nonlinear and therefore hard to solve. Note that we can compare $V^*(x)$ to a potential and g_{eff} to an effective interaction constant. Then, this equation has a similar form as the Gross-Pitaevskii equation, but includes the extra term $J(x)$ Plots of both $V^*(x)$ and $J(x)$ are shown in figure 12. Note that in the figure, $J(x)$ is antisymmetric. This will also cause some

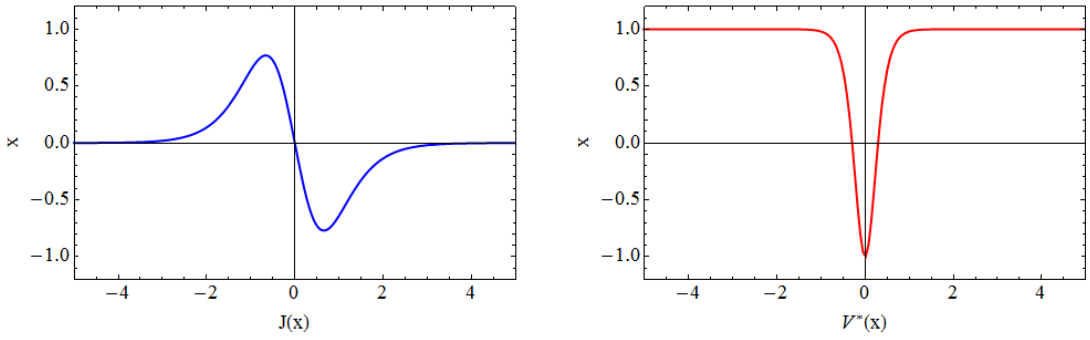

Figure 12 – In the left figure, a possible plot of $J(x)$ is shown. Note that this is an antisymmetric function. In the right figure, $V^*(x)$ is shown. This function is symmetric.

antisymmetry in the solution for $\psi_+(x)$. Luckily, $J(x)$ goes to zero for both very high and very low values of x, and thus we expect $\psi_+(x)$ to behave like the constant function $\psi_+ = \sqrt{\frac{\mu_0}{g_0}}$. We can therefore impose the following boundary conditions.

$$\begin{aligned} \psi_+(\pm\infty) &= \sqrt{\frac{\mu_0}{g_0}} \\ \frac{\partial \psi_+}{\partial x}(\pm\infty) &= 0 \end{aligned} \tag{74}$$

Solving this differential equation numerically could be a good starting point for a follow-up research on this topic. This will give some further information about the interface as well as show for which conditions earlier approximations of this interface are valid.

5 Conclusion

In this thesis we started by deriving some general properties of Bose-Einstein condensates. Using the Bose-distribution we were able to derive the critical temperature as given in equation 9. From this equation we can conclude that Bose-Einstein condensation can occur at non-zero temperatures for some potentials such as the harmonic potential in 3D. However, the same harmonic potential in 1D would require that $T = 0$, such that all our calculations in one dimension with the harmonic potential could only happen at the absolute zero temperature. Expanding the theory to 3D could improve the compatibility with the experimental situation. Furthermore the Gross-Pitaevskii equation was derived together with a free energy functional for Bose-Einstein condensates. We found that interactions play an important role in in these equations. In the case of spinor Bose-Einstein condensates in which there are spin degrees of freedom, the different interactions between different spin states causes either mixing or demixing of these states.

Subsequently the case of spinor BEC with $F = 1$ such that there are $m_F = -1$, 0 and 1 particles were considered in Thomas-Fermi approximation. In this approximation the kinetic terms are neglected, since we assume they are relatively small compared to the interaction terms for a BEC. We found that in the case of sodium, the antiferromagnetic case, there was no mixing between the $m_F = \pm 1$ state and the $m_F = 0$. On the other hand we found that in the ferromagnetic case there are mixtures of $m_F = 1$ with $m_F = 0$ and also $m_F = -1$ with $m_F = 0$, but the $m_F \pm 1$ states do not mix. We then considered the case in which a sample was prepared in which there are only spin 0 and spin -1 particles, as is the case we are most interested in. This translated into mixed states of $m_F = 0$ and -1 for the ferromagnetic case, and demixing for the case of sodium. We calculated the density profiles of both spin states from which we are also able to calculate the total number of particles. This is a known quantity in experiments.

The density profiles however contained some discontinuities in the transition between phases. This is a product of the Thomas-Fermi approximation that was used to derive these density profiles and we have to conclude that this approximation is not valid at these interfaces. We then proceeded to find density profiles without using the Thomas-Fermi approximation. This gave us the solutions given in equation 70. Increasing the factor ξ in this equation makes the interface smaller, and thus we can say that $1/\xi$ is proportional to the penetration depth of this interface. Therefore, for the Thomas-Fermi approximation to be accurate, we need the spin domains to be relatively big compared with this penetration depth, else our solutions will be governed the kinetic terms in the free energy equation. Finally a differential equation was derived that could be solved in further research to check the validity of the approximations made on the interfaces as well as give a better approximation of this interface.

References

[1] P. Panahi Thermodynamic Properties of F= 1 Spinor Bose-Einstein Condensate

[2] Website with general information about physics, viewed on 23-12-2015 http://hyperphysics.phy-astr.gsu.edu/hbase/optmod/lascool.html

[3] Image from the Australian national university website, taken on 09-01-2015. http://sciencewise.anu.edu.au/articles/qed

[4] Image from the university of Michigan website, taken on 09-01-2015. http://cold-atoms.physics.lsa.umich.edu/projects/bec/evaporation.html

[5] J. Jiang et al. *A simple and efficient all-optical production of spinor condensates*

[6] Image from Wikipedia page on Zeeman splitting, taken on 29-12-2014. http://en.wikipedia.org/wiki/Zeeman_effect

[7] C.J. Pethick, H. Smith; *Bose-Einstein condensation in dilute gases*

[8] Article on Bose-statistics, viewed on 13-11-2014 http://en.wikipedia.org/wiki/Bose%E2%80%93Einstein_statistics#Derivation_from_the_grand_canonical_ensemble

[9] W. Ketterle - *SPINOR CONDENSATES AND LIGHT SCATTERING FROM BOSE-EINSTEIN CONDENSATE*

[10] J. Stenger, S. Inouye, D. M. Stamper-Kurn, H.-J. Miesner, A. P. Chikkatur and W. Ketterle- *Spin domains in ground-state Bose-Einstein condensates*

[11] S. Knoop, T. Schuster, R. Scelle, A. Trautmann, J. Appmeier, and M. K. Oberthaler - *Feshbach spectroscopy and analysis of the interaction potentials of ultracold sodium.*- (http://arxiv.org/pdf/1102.0572v1.pdf)

[12] Article on GPE, viewed on 15-10-2014. http://arxiv.org/pdf/1301.2073v1.pdf